

**GRANITIC PEGMATITES OF THE O'GRADY BATHOLITH, N.W.T., CANADA:
A CASE STUDY OF THE EVOLUTION OF THE ELBAITE SUBTYPE
OF RARE-ELEMENT GRANITIC PEGMATITE**

T. SCOTT ERCIT[§]

Canadian Museum of Nature, P.O. Box 3443, Station D, Ottawa, Ontario K1P 6P4, Canada

LEE A. GROAT

Department of Earth and Ocean Sciences, University of British Columbia, Vancouver, British Columbia V6T 1Z4, Canada

ROBERT A. GAULT

Canadian Museum of Nature, P.O. Box 3443, Station D, Ottawa, Ontario K1P 6P4, Canada

ABSTRACT

The first confirmed Canadian occurrence of the elbaite subtype of rare-element granitic pegmatite has been encountered within the O'Grady batholith, approximately 100 km NNW of Tungsten, N.W.T. The batholith, part of the Selwyn plutonic suite, is a mesozonal, hornblende-bearing, metaluminous composite intrusion with lesser amounts of pegmatitic granite and felsitic satellite dykes. On the whole, pegmatite bodies show a mildly NYF-type geochemical and mineralogical signature (allanite- and magnetite-bearing), but in the region of the pegmatitic granite, they grade toward a distinct LCT-type signature (elbaite-bearing). The melts parental to the pegmatite bodies were more voluminous, more alkaline, less aluminous and less reduced than is the norm for melts parental to LCT-type pegmatite. Differentiation of these melts sequentially produced hornblende granite, pegmatitic leucogranite and pegmatite, as shown by major-, minor- and trace-element geochemistry of K-feldspar, plagioclase, micas, tourmaline, amphibole and a variety of accessory phases. Lithium-mineralized pegmatite is recognized by the presence of multicolored elbaite, by lepidolite, and in the diversity of characteristic accessory phases such as danburite, hambergite, stibiocolumbite, pollucite, a nanpingite-like mineral, and bismutite. The various stages of the evolution of the batholith can be well documented in similar variations in mineral chemistry, and result in one of the few well-characterized case studies of the elbaite subtype.

Keywords: granitic pegmatite, elbaite subtype, principal components analysis, melt evolution, accessory minerals, O'Grady batholith, Selwyn plutonic suite, Northwest Territories.

SOMMAIRE

Nous décrivons le premier exemple canadien d'une pegmatite granitique à éléments rares du sous-type à elbaïte; il fait partie du batholithe de O'Grady, situé environ 100 km au nord-nord-ouest de Tungsten, Territoires du Nord-Ouest. Le batholithe, membre de la suite plutonique de Selwyn, résulte de la mise en place mésozonale de venues métallumineuses, à hornblende, avec une proportion moindre de granite pegmatitique et de filons satellites felsiques. En général, les masses de pegmatites possèdent des caractéristiques rappelant une filiation géochimique et minéralogique de type NYF (à allanite et magnétite), mais près de l'endroit où affleure le granite pegmatitique, elles montrent une gradation vers une composition distincte de type LCT (roches à elbaïte). Le magma parental de cette suite de pegmatites était plus volumineux, plutôt alcalin, moins alumineux et moins réduit que la norme pour les magmas responsables de la formation des pegmatites de type LCT. La différenciation de ces liquides a produit la séquence allant de granite à hornblende, leucogranite pegmatitique et pegmatite, comme le démontre les éléments majeurs, mineurs et en traces dans le feldspath potassique, le plagioclase, les micas, la tourmaline, l'amphibole et une variété de phases accessoires. La pegmatite minéralisée en lithium se distingue par la présence d'elbaïte multicolore, de lépidolite, et d'accessoires comme la danburite, la hambergite, la stibiocolumbite, la pollucite, un minéral semblable à la nanpingite, et

[§] E-mail address: sercit@mus-nature.ca

bismutite. Les divers stades de l'évolution du batholithe sont documentables par les variations semblables dans la composition des minéraux, ce qui mène à un des rares exemples bien documentés d'une pegmatite granitique du sous-type à elbaïte.

(Traduit par la Rédaction)

Mots-clés: pegmatite granitique, sous-type à elbaïte, analyse des composantes principales, évolution du magma, minéraux accessoires, batholithe de O'Grady, suite plutonique de Selwyn, Territoires du Nord-Ouest.

INTRODUCTION

In 1993, we launched a field program directed at delineating rare-element granitic pegmatite fields of the northern Canadian Cordillera. One of the results of our efforts was the discovery of the first confirmed Canadian occurrence of the elbaite subtype of rare-element granitic pegmatite, in the vicinity of the O'Grady Lakes, Northwest Territories. The occurrence hosts abundant bodies of miarolitic lithium-mineralized pegmatite with euhedral and locally gemmy elbaite (Fig. 1). In our literature research, we discovered that the relatively newly defined elbaite subtype (Novák & Povondra 1995) is only moderately well characterized in terms of its geochemistry, and even less so in terms of its petrogenesis. Given this situation and our good fortune in encountering an occurrence of the elbaite subtype with a

well-exposed sequence of magmatic precursors to the pegmatites, we decided that a relatively thorough examination of the occurrence was called for, with the hopes of unveiling much of its evolutionary history.

REGIONAL SETTING

The pegmatite field and its hosts lie within the Selwyn Basin of the northern Canadian Cordillera. The general geology of the basin has been outlined by Gordey & Anderson (1993). The area is underlain by weakly metamorphosed sedimentary rocks of late Precambrian to Triassic age. Regional Jurassic–Cretaceous deformation resulted in small- to large-scale northwest-trending folds and tectonic thickening up to three times original (Cecile 1984). Most plutonic rocks of the region belong to the mid-Cretaceous, calc-alkaline Selwyn



FIG. 1. Pale pink elbaite on microcline, O'Grady batholith.

suite, consisting of metaluminous to peraluminous granitic rocks that Gordey & Anderson (1993) subdivided into three groupings: hornblende-bearing plutons, two-mica plutons, and transitional plutons with attributes intermediate to these extremes. Mortensen *et al.* (1997) represented each grouping as a distinct plutonic suite, hence their terminology: Tombstone suite (hornblende-bearing), Tungsten suite (two-mica), and Tay River suite (transitional). The Tay River suite (97 ± 1 Ma) would seem to be older, and thus hardly "transitional" to the two other suites (*cf.* 91.5 ± 1 Ma for the Tombstone suite), that may be comagmatic (Mortensen *et al.* 1997, Heffernan & Mortensen 2000). Mineralogical, geochemical, and textural data indicate that the peraluminous, two-mica plutons are the most evolved members of the broader Selwyn suite. Gordey & Anderson (1993) suggested an epizonal to mesozonal depth of emplacement for the plutons. Contact aureoles are typically andalusite- and biotite-bearing; the first appearance of andalusite occurs within half a kilometer of intrusive contacts. Granitic pegmatites are associated with some of the plutons of the suite, both with large, metaluminous hornblende-bearing intrusions like the O'Grady batholith, and smaller peraluminous hornblende-free ones like the W-skarn-associated Clea and MacTung plutons (Anderson 1983).

GEOLOGY OF THE O'GRADY BATHOLITH

General

The O'Grady batholith is located in the Sapper Ranges of the Selwyn Mountains, approximately 100 km north-northwest of the town of Tungsten, in the western Northwest Territories (Fig. 2). It is a 94 Ma (weighted mean K–Ar age), hornblende-bearing, alkali-feldspar-rich composite intrusion (Anderson 1983). The batholith, 270 km², consists of a megacrystic hornblende granite (hornblende quartz syenite of Gordey & Anderson 1993), a marginal, massive, equigranular hornblende–biotite granodiorite, and a foliated transitional phase between the two (Fig. 3). The hornblende granite (Fig. 4a) is remarkably homogeneous over the region investigated; the only obvious variations involve the modal abundances of hornblende and mafic enclaves. Late-stage differentiates include heterogeneous pegmatitic granite hosted within the hornblende granite, and peraluminous felsitic dykes satellitic to the batholith.

The whole-rock geochemistry of the O'Grady batholith has been described by Gordey & Anderson (1993), augmented slightly by Groat *et al.* (1995). The batholith is much less silicic than two-mica plutons in the Selwyn suite (mean SiO₂ = 65.1%, *cf.* 72.5% for two-mica plutons), is metaluminous (mean Shand index of 0.80), diopside-normative, and has mixed I- and S-type characteristics. Some mean trace-element values are noteworthy: Li 54, B 202, Rb 325, [Cs 21], Be 7, F 0.12, Nb 24, Y 27, La 110, Yb undetected, [Ga 14], Sn

8, W 8, Zr 217, U 18 ppm, as are key element-ratios: K/Rb 151, K/Ba 77, Ba/Sr 2.2, Mg/Li 255 (values in brackets represent single measurements). Although the batholith would seem unexceptional in terms of its major-element composition and some trace-element signatures, *e.g.* Mg/Li, it displays some evidence of a highly fractionated nature, including low K/Rb values and high light-lithophile-element contents relative to averages for granitic rocks. On the basis of typical tectonic discriminant plots (Pearce *et al.* 1984, Pearce 1996), its composition falls at the overlapping margins of fields for granites in syn- to post-collisional settings, as might be expected from the tectonic setting of the Selwyn plutonic suite (Gordey & Anderson 1993, Woodsworth *et al.* 1992).

Pegmatitic granite

This unit has been previously described as a zone of "alaskite", aplite and pegmatite intrusions or as a pegmatite–aplite belt (*e.g.*, Anderson 1983, Groat *et al.* 1995). However, it is better described as pegmatitic granite (Fig. 4b), consisting mostly of fine-grained leucogranite with abundant pegmatitic segregations and offshoots. It is exposed in a 10-km-long belt along the western margin of the intrusion, with a maximum exposed width of 1 km, and is statistically the same age as less-evolved phases of the batholith (Hunt & Roddick 1987, Gordey & Anderson 1993). Lithium mineralization is localized within a 1-km long section of the belt

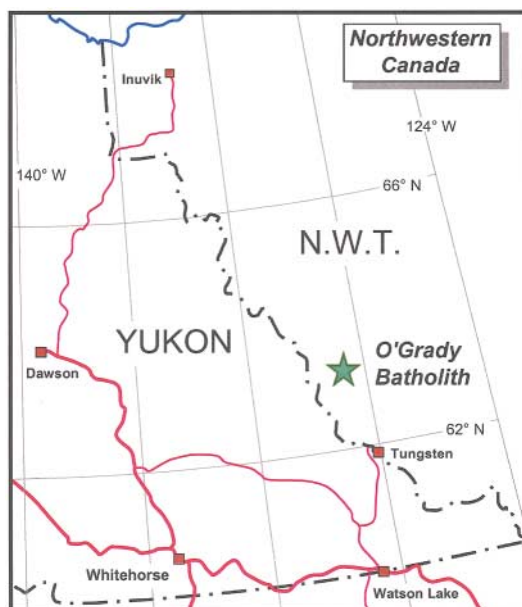


FIG. 2. Location map.

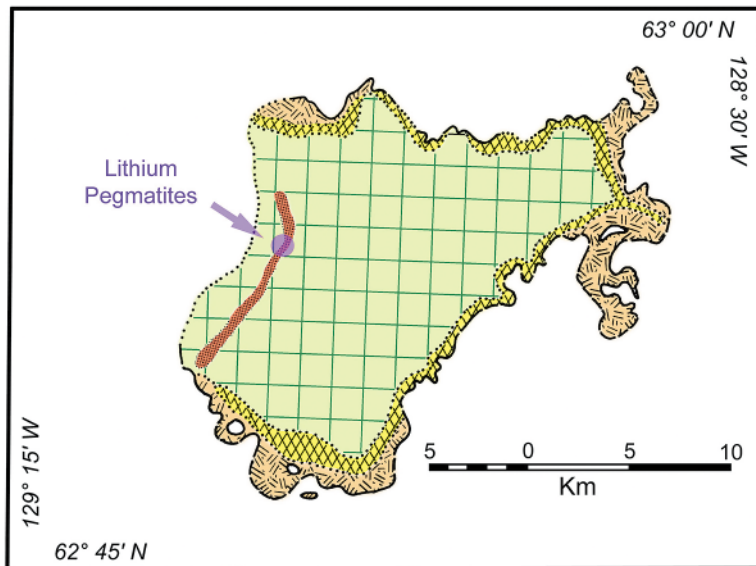


FIG. 3. Geology of the O'Grady batholith (after Anderson 1983). Coarse cross-hatching: hornblende granite, herring-bone pattern: marginal granodiorite, fine cross-hatching: transitional phase; stippling: pegmatitic granite.

(Fig. 3); the majority of our field work focused on this section. The limits to the lithium-mineralized region consist of a post-emplacement fault to the southeast, cirque valleys to the north and east, and the disappearance of outcrop under overburden to the west (Ericit *et al.* 1998).

Although approximately horizontal and linear, the contacts between the pegmatitic granite and the host hornblende granite are undulose over a scale of a few hundred meters, and rafts and screens of hornblende granite within pegmatitic granite are relatively common. In the vicinity of the lithium-mineralized region, the average exposed thickness of the pegmatitic granite is close to 20 m, with a maximum of 80 m. On the basis of available exposures, two interpretations exist for the geological relationship between the pegmatitic granite and the hornblende granite. One is that current exposures represent near-roof marginal contacts of a potentially larger body of granite, and that hornblende granite "interlayers" are merely rafted sheets and blocks within the roof region. As an alternative, the pegmatitic granite exists as a small-volume series of sills occupying horizontal fractures in the hornblende granite.

The relationship between pegmatite bodies and the leucogranite varies considerably, but can be considered as a spectrum of styles between two extremes. We have labeled one extreme *poorly segregated*, in which pegmatites occur as small (typically less than 0.25 m long), irregular to lens-like segregations within the

leucogranite (*e.g.* Fig. 4b). We designate the other extreme as *segregated*, which occurs as discrete, well-zoned pegmatitic sills. The segregated pegmatites occur both within the pegmatitic granite and peripheral to it, *i.e.*, within the hornblende granite.

Most pegmatite bodies show simple, vertically asymmetric zoning. Where visible, the outermost unit is a commonly irregular, mm-scale, plagioclase-rich border unit. This is concentrically followed by a graphic zone that is typically thicker and coarser-grained in its upper portion than in the basal portion. The basal portion consists of medium-grained, locally graphic K-feldspar, plagioclase and quartz \pm accessory tourmaline (schorl), and biotite. The upper portion has a similar assemblage of minerals to the basal portion, but with an order of magnitude coarser grain-size, and a much more obviously graphic texture. The average grain-size of crystals in this zone is generally larger than crystals of the pocket zone. K-feldspar crystals are commonly pink, whereas K-feldspar in the basal portion is noticeably whiter, and locally amazonitic; we have often used K-feldspar color as a field indicator of pocket location. The most central zone is a pocket zone, consisting of well-formed crystals of K-feldspar, quartz (commonly smoky), pale blue platy plagioclase, elbaite, lepidolite, and a variety of accessory phases.

Miarolitic cavities (Fig. 4b) are a common feature of pegmatite bodies of the O'Grady batholith, but are absent in the hornblende granite. They range in volume



FIG. 4. Photographs of selected phases of the O'Grady batholith. (a) Crowded megacrystic hornblende granite with a mafic enclave (central). Megacrysts consist of K-feldspar; plagioclase, hornblende and quartz form the finer-grained matrix. (b) Pegmatitic granite showing a small pocket with a crystal of white K-feldspar. The contact with surrounding hornblende granite is visible in the upper quarter of the photograph.

from a few cm³ to several m³, and are lens-like in shape, elongate in a horizontal plane conformable with sill attitude. Virtually all pockets host well-formed crystals that range from microscopic to over 15 cm in size, depending upon a number of factors such as pocket size, mineral species and the concentration of elements like lithium and boron during pocket formation. Many pocket crystals, *e.g.* of K-feldspar and quartz, are etched, evidence of corrosion by the fluid phase at some stage. Most near-surface pockets have suffered the effects of exposure and frost shattering; crystals are typically dislodged from the pocket wall. Pockets are in some cases filled with debris washed in from higher elevations *via* fracture systems. As such, the finer-grained, void-filling contents of near-surface pockets cannot be considered to be representative of the latest stages of pocket formation.

PETROGRAPHY

Hornblende granite

This unit varies from hornblende granite to hornblende quartz syenite (Gordey & Anderson 1993; R.G. Anderson, pers. commun.). As all of our samples, and all published modal analyses of the unit (Hunt & Roddick 1987) show it to be hornblende granite by IUGS standards, we refer to it as such. The unit consists of pale grey subhedral to euhedral, micropertthitic K-feldspar megacrysts to 1 cm, in a fine-grained matrix of generally white subhedral plagioclase, colorless subhedral quartz and dark green euhedral hornblende, with minor amounts of brown biotite. The core of plagioclase crystals is euhedral and calcic (andesine to sodic labradorite), and the rim is typically subhedral and

sodic (albite). The hornblende is pleochroic and is typically compositionally unzoned. Common accessory phases are titanite, magnetite, zircon, an apatite-group mineral and thorite; much less common are allanite-(Ce), ilmenite, scheelite, and relict clinopyroxene (calcic augite). Many of the accessory phases are hosted within hornblende. Minor propylitic alteration manifests itself as partial replacement of calcic plagioclase by sodic plagioclase and epidote, and of hornblende by chlorite.

Leucogranite

The fine-grained portion of the pegmatitic granite consists of generally equigranular K-feldspar, quartz and albite; the mean grain-size is in the range of 0.5 to 2 mm. The K-feldspar is micro- to cryptoperthitic and generally subhedral to euhedral. Plagioclase is euhedral to subhedral, and consists of a calcic core (oligoclase–andesine) and a sodic (albite) rim. The core area occasionally shows partial replacement by sodic plagioclase,

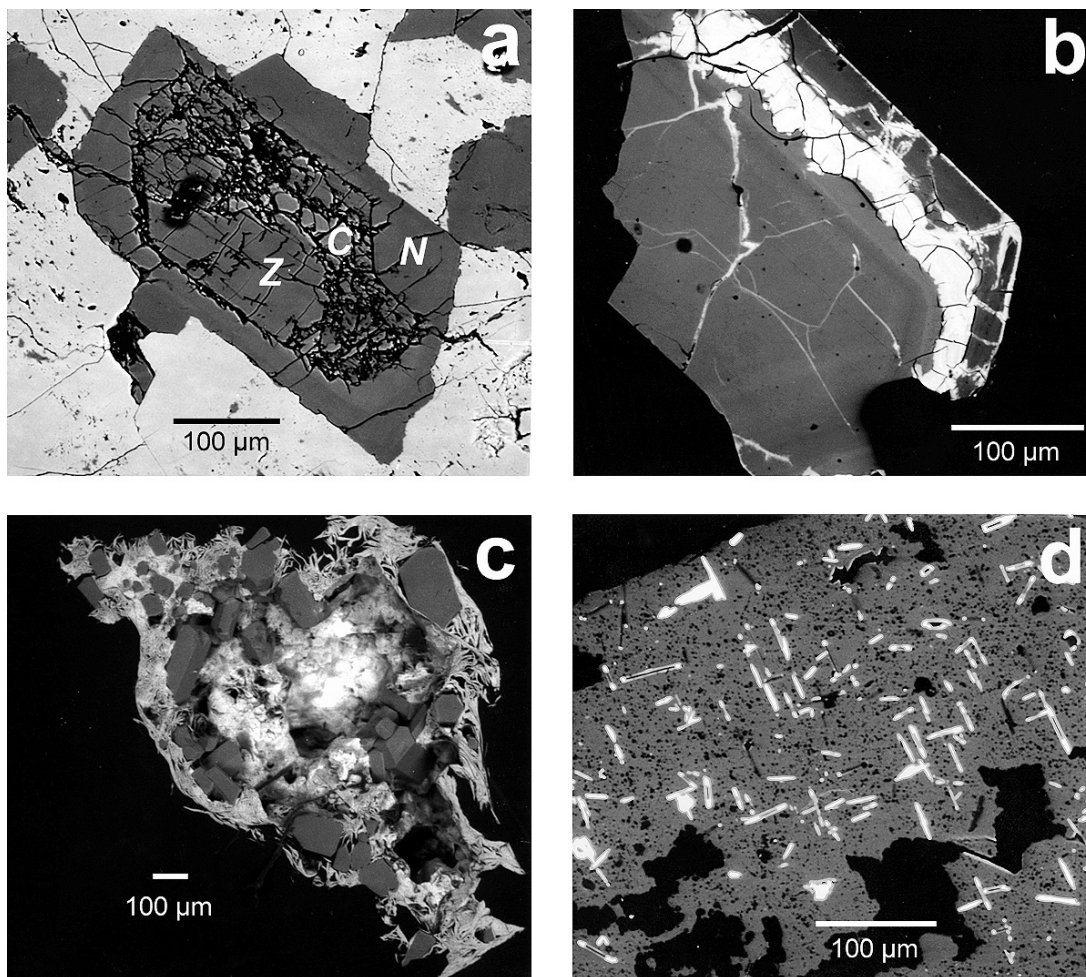


FIG. 5. Back-scattered electron (BSE) images of late mineralization in O'Grady pegmatite. (a) Heavily fractured, Cs-bearing chabazite (Z) partly replacing calcic plagioclase (C), but sodic plagioclase at the rim (N) remains unaltered. (b) Bismuthian plumbopyrochlore (bright) replaces primary pyrochlore. Note desiccation cracks in plumbopyrochlore. (c) Small pocket with crystals of colorless elbaite (equant, grey) and nanpingite-like mineral (bladed, brighter grey). (d) Pervasive alteration of a pocket K-feldspar crystal (grey) to a nanpingite-like mineral (bright). Note pithy texture of K-feldspar.

or by other mineral phases such as zeolites (Fig. 5a). The zeolitic alteration (chabazite-Ca) is a subsolidus phenomenon, as evidenced by elevated trace concentrations of Cs in samples (400 to 1200 ppm). Quartz is generally anhedral, but in some bodies of apparently aplitic leucogranite, it is subhedral to euhedral. In these bodies, tourmaline occurs in late plagioclase-rich clots, and is virtually invariably interstitial to the feldspars. Accessory phases are generally an order of magnitude finer grained than the main phases. The most common accessory phases are biotite, magnetite and titanite. Somewhat less common are zircon, thorite, magmatic fluorite, ilmenite-pyrophyranite solid solution and an apatite-group mineral. Allanite-(Ce), rutile, scheelite, yttrropyrochlore-(Y), xenotime-(Y), monazite-(Ce), fergusonite-(Y) are rare accessory phases. With very rare exceptions (a single hornblende xenocryst), amphibole is absent. See Appendix 1 for a representative photo-mosaic of this rock.

Granitic pegmatite

Pegmatitic segregations consist of generally coarse-grained K-feldspar, plagioclase and quartz. Most pegmatite displays a mild NYF-like (*Nb-Y-F* enriched) signature, as shown by the relative abundance of magnetite and lanthanon-bearing minerals and the absence of minerals typical of LCT (*Li-Cs-Ta* enriched) pegmatite (Table 1). K-feldspar samples from the upper graphic zone of segregated pegmatite can achieve a grain size on the order of several decimeters. K-feldspar in the lower graphic zone is generally finer grained, and is locally amazonitic, particularly within the lithium-mineralized region. Pocket K-feldspar crystals are generally less than 10 cm in size. K-feldspar samples are micropertthitic to perthitic, with well-developed albite lamellae, and on the whole tend to be darker colored in NYF pegmatite than in lithium-mineralized pegmatite. Graphic K-feldspar and quartz, plagioclase

and quartz, and tourmaline and quartz can be found in the graphic zones. In samples from the graphic zones, tourmaline tends to be either graphic or interstitial to other phases, and invariably iron-rich. Samples of tourmaline from the pocket zone range from schorl to elbaite. The root or core of otherwise transparent crystals of elbaite commonly consists of black, opaque schorl. Boron activity was relatively high during pocket formation, as is indicated by the overall abundance of tourmaline and, in LCT pegmatite, by the common appearance of danburite, and sporadic appearance of hambergite, not beryl, as the main carrier of beryllium. Also, microscopic druses of gem elbaite coating K-feldspar are common in the lithium-mineralized region. In exceptional cases, partly tourmalinized pocket K-feldspar can be found, evidence of local boron metasomatism, which in turn illustrates the extremes reached in terms of boron activity. These latest fluids occupying the pockets are locally highly enriched in cesium. In many cases, sparse to pervasive alteration of K-feldspar to a nanpingite-like mineral is present (Fig. 5d). Accessory phases in the pegmatite bodies (Table 1) include rock-forming pollucite (*i.e.*, not a pocket phase).

Satellitic dykes

The satellitic dykes are texturally and compositionally felsite. Crypto- to micropertthitic K-feldspar, plagioclase and quartz are the main phases. The average grain-size is only a fraction of a millimeter. The peraluminous composition of the dykes is reflected in their accessory minerals; they are muscovite- and tourmaline-bearing. Other accessory phases include monazite-(Ce), xenotime-(Y), rutile, zircon and bismutopyrochlore.

MINERAL CHEMISTRY

Analytical methods

Samples were chemically analyzed at the Canadian Museum of Nature with a JEOL 733 electron microprobe with Tracor Northern 5500 and 5600 automation. The operating voltage was 15 kV, the beam current, 20 nA. The beam diameter was varied from a point focus to 20 μm depending upon sample stability. All samples were examined first by back-scattered electron (BSE) imaging and qualitative energy-dispersion analysis. Data for standards were collected for 50 s or to 0.25% precision (1σ level), whichever was attained first. Similarly, data for samples were collected for 25 s or to 0.5% precision, with the exception of geochemically useful trace elements, which were counted for longer times to improve detectability. An element was considered to be detected if it attained a significance level of 4σ or better. Data reduction was done with conventional ZAF routines for common silicate minerals; for compositionally complex species, we used the PAP routine in the

TABLE 1. MINERALOGY OF PEGMATITE BODIES, O'GRADY BATHOLITH, N.W.T.

Minerals found in all types	Minerals typical of NYF bodies	Minerals typical of LCT bodies
Quartz	Magnetite	Elbaite
Microcline	Allanite-(Ce)	Polyolithionite-lepidolite
Plagioclase	Allanite-(La)	Stilbite
Schorl-dravite	Thorite	Danburite
Muscovite	Monazite-(Ce)	Hambergite
Biotite series		Pollucite
Ferro-axinite		Nanpingite-like mica
Titanite		Pyrochlore-group minerals
Zircon		Stibiocolumbite
Ilmenite		Scheelite
Pseudorutile		Bismutite
Apatite		Cassiterite
Opal		
Xenotime-(Y)		
Fluorite		

Each column is approximately in order of decreasing abundance.

computer program XMAQNT (C. Davidson, CSIRO, pers. commun.). A wide variety of natural and synthetic standards, too numerous to list here, was used in mineral analysis. Compositional data for the most common phases are available from the Depository of Unpublished Data, CISTI, National Research Council, Ottawa, Ontario, Canada K1A 0S2; selected compositional data for other phases are tabulated here.

For most minerals, summary details about formula calculation are contained in the tables of this paper. However, for tourmaline, further detail is required. Tourmaline compositions were originally calculated on a basis of 31 total anions assuming (i) all Fe as Fe^{2+} , (ii) stoichiometric amounts of B, and (iii) $(\text{OH} + \text{F}) = 4 \text{ apfu}$ (atoms per formula unit). Lithium-bearing samples were quickly detected by two prerequisite features: high content of $^{\text{VI}}\text{Al}$ and significantly deficient sum of octahedrally coordinated cations. With both boron and lithium unmeasurable with an electron microprobe, others have chosen to calculate the amount of lithium iteratively (Burns *et al.* 1994, Selway *et al.* 1999). However, Li and Li_2O are easily calculated in a single step by ignoring the component B_2O_3 in the tourmaline formula, thereby using a basis of 26.5 total anions and 15 tetrahedral and octahedral cations for the calculation (B and B_2O_3 can then be calculated in a second step by using this value of Li_2O in the calculation, on the usual basis of 31 total anions). In addition to the above, a number of non-lithian tourmaline samples gave compositions that are subaluminous ($^{\text{VI}}\text{Al} < 6 \text{ apfu}$). For these, a *minimum* estimate of Fe^{3+} was calculated from total iron by

assuming octahedral $(\text{Al} + \text{Fe}^{3+}) = 6 \text{ apfu}$; to preserve charge balance, a matching amount of OH was converted to O. However, a small number of these cases and a number of normally aluminous (*i.e.*, $\text{Al} > 6 \text{ apfu}$) compositions had significantly excessive cation sums, that also required conversion of Fe^{2+} to Fe^{3+} , this time by normalizing on a total of 15 octahedral and tetrahedral cations per $27(\text{O}) + 4(\text{OH}, \text{F})$ anions to give a *maximum* estimate of Fe^{3+} . Although this procedure might seem terribly complex, and therefore a bit contrived, the reader should understand that subaluminous tourmaline is extremely rare, hence this approach has not been considered or discussed previously.

Feldspar

Plagioclase is strongly variable in composition, but is on the whole quite calcic. The composition ranges from An_{52} to An_2 in hornblende granite, with a volume-weighted mean of An_{30} . It ranges from An_{32} to $\text{An}_{0.2}$ in leucogranite and felsitic satellite dykes, with a weighted mean of An_{18} . And it ranges from An_{28} to An_0 in pegmatite, with a weighted mean of An_5 . In addition, all lithologies show a composition gap in terms of calcium content (Fig. 6). The gaps can be correlated with core (calcic) and rim (less calcic) compositions of crystals. The calcic compositions of some pegmatite-hosted plagioclase are atypical of rare-element pegmatites. A striking feature of both plagioclase and K-feldspar samples is the complete absence of detectable P (<120 ppm under the operating conditions of the present study). This

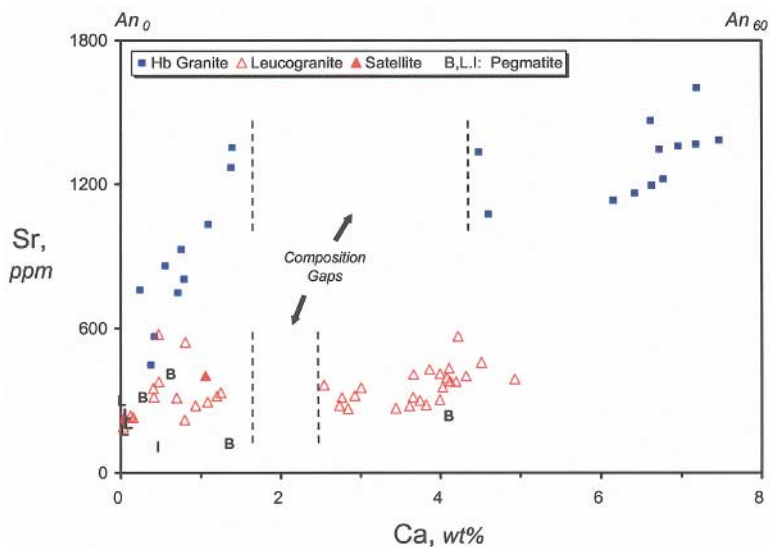


FIG. 6. Variation of Sr versus Ca in plagioclase. Composition gaps correspond to calcium variation. Calcic compositions correspond to the core of crystals; sodic compositions correspond to overgrowth compositions.

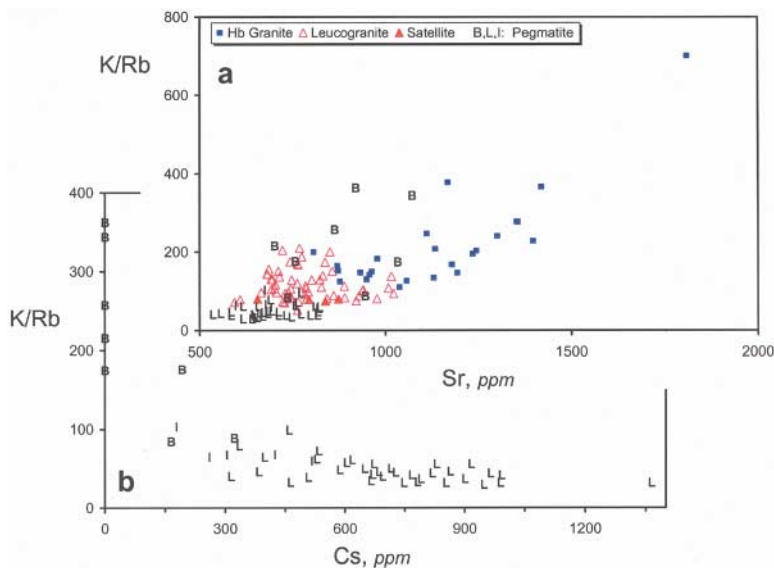


FIG. 7. Geochemical data for K-feldspar. (a) K/Rb versus Sr. The lack of scatter in this plot in part reflects the relatively young age of the batholith and its derivatives (*ca.* 94 Ma). (b) K/Rb versus Cs for samples from pegmatite. Points near Cs = 0 do not have detectable Cs, but are plotted to show K/Rb variation.

is atypical for feldspar samples from moderately to highly fractionated granites and pegmatites, which can host up to 1.2 wt% P₂O₅ (London *et al.* 1990). Clearly, phosphorus activity remained extremely low throughout the entire history of fractionation of the batholith, and calcium activity was sufficiently high to extract the negligible phosphorus from the melt in the form of apatite.

Potassium feldspar is the most common mineral of all major rock types. In terms of major elements, it is unremarkable; compositions range from Or₈₆ to Or₉₉, and are similar for all rock types. Crystals from all units show normal zoning, with a rim depleted in Ba and enriched in Rb and Cs (where detectable). Several broad aspects of the trace-element chemistry are worthy of note. Figure 7a is a plot of the K/Rb value versus Sr for K-feldspar compositions from all rock types. The K/Rb values for the hornblende granite are atypically low (mean: 215), and overlap and grade into the range for leucogranite and satellite dykes (mean: 210), which also overlaps and grades into the range for pegmatite (mean barren: 215; mean lithium-mineralized: 45). Clearly, most of the fractionation of K from Rb occurred during pegmatite generation. As compared to K/Rb, strontium shows considerably less overlap between rock types, and displays much more gradational behavior over the entire span of crystallization of the batholith: mean hornblende granite: 1150 ppm, mean leucogranite and satel-

lite dyke: 785 ppm, mean barren pegmatite: 880 ppm, mean lithium-mineralized pegmatite: 695 ppm. Although data for barium are not shown here, its behavior is similar to that of Sr. However, Ba behaves more compatibly, so that by the time of pegmatite crystallization, it is undetectable (<200 ppm under the present operating conditions). Figure 7a also attests to the relatively young age of the pegmatites. Granitic pegmatites from older pegmatite belts show either no correlation between K/Rb and Sr, or where showing a trend, tend to display a late reversal in the behavior of Sr (Clark & Černý 1987). Quite clearly, most of the Sr in O'Grady samples is non-radiogenic, and any post-crystallization migration of Sr has not been significant enough to obscure the original Rb–Sr fractionation trend.

Figure 7b illustrates the behavior of the larger alkali cations during the evolution of the pegmatite-forming melts. Cesium behaves strongly incompatibly; it is undetectable in all other rock types (<200 ppm), and only starts to be detected in K-feldspar from some bodies of barren pegmatite and from all bodies of lithium pegmatite. There is a clear and continuous variation in the K/Rb value and Cs content of K-feldspar from barren pegmatite (B: devoid of lithium minerals), to intermediate pegmatite (I: anomalously geochemically and mineralogically evolved, but devoid of lithium minerals), and finally lithium-mineralized pegmatite (L). Some pegmatite bodies with K-feldspar samples near the Cs-rich end

of this range also host pollucite or show evidence of subsolidus alteration of K-feldspar to a nanpingite-like mineral.

Tourmaline

The general formula of tourmaline is $X_{0-1}Y_3Z_6(T_6O_{18})(BO_3)_3V_3W$, where X is a large cation (Na, Ca or K), Y and Z are octahedrally coordinated cations (typically Al, Li, Mg, and transition metals), T is a tetrahedrally coordinated cation (Si, Al or, very rarely, B), and V and W are OH, F or O (Hawthorne & Henry 1999). Compositional variability in tourmaline from the O'Grady batholith is most obviously expressed in its color; subtle variations (Table 2) have no physical expression. All tourmaline outside of the lithium-mineralized region is black, and mostly a schorl–dravite solid solution. Tourmaline inside the lithium-mineralized region is mostly black, but pink, red, yellow-brown and rare green crystals indicate the presence of fluorine-rich elbaite. Virtually all elbaite occurs in pockets; crystals are glassy, euhedral and strongly color-zoned. At their most extreme, color-zoned crystals may have a dark core verging on lithian schorl, colorless outer surfaces approaching transition-metal-free elbaite–rossmanite solid-solution, and a multitude of color bands and compositions in between. Figure 8 illustrates typical color and compositional zoning in a section cut perpendicular to the c axis. Most of the zoning follows well-recognized patterns: from core to rim, (i) transition metal contents decrease, with Mn lagging behind Fe, (ii) Li and ^{VI}Al increase, and (iii) ^{IV}Al increases. Some anomalous behavior exists; in particular, F decreases and Ca increases. Late enrichment in both Ca and F of pegmatitic tourmaline has been taken as a possible indication of incompatible behavior of Ca in late melts and fluids consequent to its formation of fluoride complexes (Tindle *et al.* 2002; *cf.* Weidner & Martin 1987). Antipathetic behavior of these elements in tourmaline from the O'Grady batholith might seem to be at odds with such a model, but only if competition between phases is ignored. For example, in an environment in which elbaite is the main sink for lithium, once lithium and fluorine activities increase to a suitable level to promote crystallization of lepidolite, F levels in elbaite should drop. Paraphrased, sympathetic behavior of Ca and F might be recognized only when the full assemblage of F-bearing minerals is considered.

The composition of tourmaline is widely variable across all of its host units in the O'Grady batholith, and as such has potential as a petrogenetic indicator. This

lar to the c axis. Most of the zoning follows well-recognized patterns: from core to rim, (i) transition metal contents decrease, with Mn lagging behind Fe, (ii) Li and ^{VI}Al increase, and (iii) ^{IV}Al increases. Some anomalous behavior exists; in particular, F decreases and Ca increases. Late enrichment in both Ca and F of pegmatitic tourmaline has been taken as a possible indication of incompatible behavior of Ca in late melts and fluids consequent to its formation of fluoride complexes (Tindle *et al.* 2002; *cf.* Weidner & Martin 1987). Antipathetic behavior of these elements in tourmaline from the O'Grady batholith might seem to be at odds with such a model, but only if competition between phases is ignored. For example, in an environment in which elbaite is the main sink for lithium, once lithium and fluorine activities increase to a suitable level to promote crystallization of lepidolite, F levels in elbaite should drop. Paraphrased, sympathetic behavior of Ca and F might be recognized only when the full assemblage of F-bearing minerals is considered.

The composition of tourmaline is widely variable across all of its host units in the O'Grady batholith, and as such has potential as a petrogenetic indicator. This

TABLE 2. SELECTED TOURMALINE COMPOSITIONS, O'GRADY BATHOLITH

	Schorl	Dravite	Uvite	Elbaite
SiO ₂ wt.%	33.71	35.66	34.27	36.81
TiO ₂	0.80	0.59	0.86	0.00
B ₂ O ₃ *	9.69	10.55	9.91	11.00
Al ₂ O ₃	26.64	30.64	24.24	41.28
V ₂ O ₅	0.00	0.00	0.08	0.00
Fe ₂ O ₃	2.75	1.44	8.17	0.00
MgO	0.20	6.56	6.96	0.00
MnO	0.00	0.07	0.08	0.21
FeO	18.99	9.42	7.29	0.00
CaO	0.60	1.63	2.65	1.96
Li ₂ O*	0.00	0.00	0.00	2.30
Na ₂ O	2.09	1.84	1.34	1.56
K ₂ O	0.04	0.05	0.06	0.00
H ₂ O*	3.03	3.12	2.56	3.04
F	0.00	0.76	0.64	1.58
O=F	0.00	-0.32	-0.27	-0.67
	98.54	101.99	98.84	99.07
Formula contents per 31 anions				
Si <i>apfu</i>	6.04	5.87	5.96	5.82
Al	0.00	0.13	0.04	0.18
T	6.04	6.00	6.00	6.00
B	3.00	3.00	3.00	3.00
Al	5.63	5.82	4.93	6.00
Fe ³⁺	0.37	0.18	1.07	0.00
Z	6.00	6.00	6.00	6.00
Ti	0.11	0.07	0.11	0.11
Al	0.00	0.00	0.00	1.51
V	0.00	0.00	0.01	0.00
Mg	0.05	1.61	1.80	0.00
Fe ²⁺	2.85	1.30	1.06	0.00
Mn	0.00	0.10	0.01	0.03
Li	0.00	0.00	0.00	1.46
Y	3.01	2.99	3.00	3.00
Ca	0.11	0.29	0.49	0.33
Na	0.73	0.59	0.45	0.48
K	0.01	0.01	0.01	0.00
X	0.85	0.89	0.96	0.81
OH	3.63	3.43	3.00	3.21
F	0.00	0.40	0.35	0.79
O	27.37	27.18	27.65	27.00

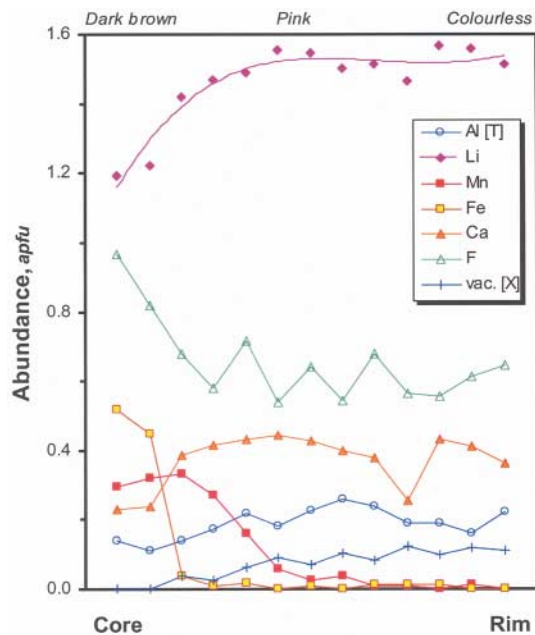


FIG. 8. Compositional zoning in a crystal of color-zoned elbaite 3 cm in diameter.

All samples are from granitic pegmatite except the dravite sample, from a felsitic satellite dyke.
* calculated for stoichiometry (as well as Fe²⁺:Fe³⁺)

potential has been recognized for other pegmatite deposits (Novák & Povondra 1995, Selway *et al.* 1999, Novák *et al.* 1999), and some geochemically useful plots have been developed. Figure 9a is one such plot illustrating variations in X-site and Y-site occupancies (understanding that variations in Li are largely reflected in Y-site Al content). The X-site occupants in tourmaline from the O'Grady batholith are typical of tourmaline from the elbaite subtype of pegmatite (Novák & Povondra 1995), *i.e.*, richer in Ca and poorer in vacancies than other lithium subtypes of the rare-element class of pegmatite (*e.g.*, Selway *et al.* 1998, 1999). However, the Y-site occupancy is unusual (Fig. 9b); in particular, schorl compositions are Fe³⁺-enriched. In lieu of what is known of Y-Z-site disorder of Mg in tourmaline (Hawthorne *et al.* 1993, Grice & Ercit 1993), it is interesting to note that the presence of Z-site Fe³⁺ in tourmaline from O'Grady is *unambiguously* indicated by the combination of subaluminous compositions, *i.e.*, with $Z\text{Al} < 6 \text{ apfu}$, and the common occurrence of T- or $\Sigma(T,Z,Y)$ -position excessive cation sums in Mg-poor schorl (*e.g.*, the composition reported in Table 2). Although Fe³⁺-enriched compositions of schorl are unusual for pegmatites of LCT geochemistry, careful scrutiny of the compositions reported in Novák & Povondra (1995) would seem to indicate that Fe³⁺-enrichment is not unusual for the elbaite subtype (*e.g.*, Řečice, Vlastějovice and Radkovice pegmatites, Czech Republic, although Novák & Povondra suggested that high Fe³⁺ at Vlastějovice is due to direct contamination from country rock, a Fe-skarn). What is unusual is the associated subaluminous bulk-composition of tourmaline from the O'Grady batholith. Schorl samples from the O'Grady batholith not only show Fe³⁺ enrichment,

they also are enriched in a povondraite $[\text{NaFe}^{3+}_3(\text{Fe}^{3+}_4\text{Mg}_2)\text{Si}_6\text{O}_{18}(\text{BO}_3)_3(\text{OH})_3\text{O}]$ component, a feature not previously recognized for granitic pegmatite-hosted tourmaline.

No consensus exists on how to examine the composition of pegmatitic tourmaline for fractionation trends, nor has any consistent set of plots been established, owing in part to the compositional complexity of tourmaline. In the absence of such consensus, we chose to use principal components analysis to represent and interpret the composition of tourmaline from the O'Grady batholith. Although rarely used to evaluate mineral geochemistry, principal components analysis is a conceptually simple and useful way to reduce the multidimensionality of complex compositional data. The technique operates by constructing *principal components*, supervariables of a sort, from the individual compositional data, on the basis of total variance of the data. In essence, the goal of the technique is to construct as few plots as possible to illustrate the maximum amount of variance. The main drawback of the technique is that the principal components may not have an immediately obvious interpretation; the investigator must scrutinize the eigenvectors or the component loadings to obtain a physically realistic interpretation of the result.

The principal components analysis was done with SYSTAT for Windows, version 10. The formula contents for each sample were used as the independent variables, less the following semidependent variables: Si, ^{VI}Al, OH and O. The analysis showed that 91% of the total variance in the data could be accounted for by two principal components, which were calculated from the variance-covariance matrix. The two principal components (PC1, PC2) are defined as:

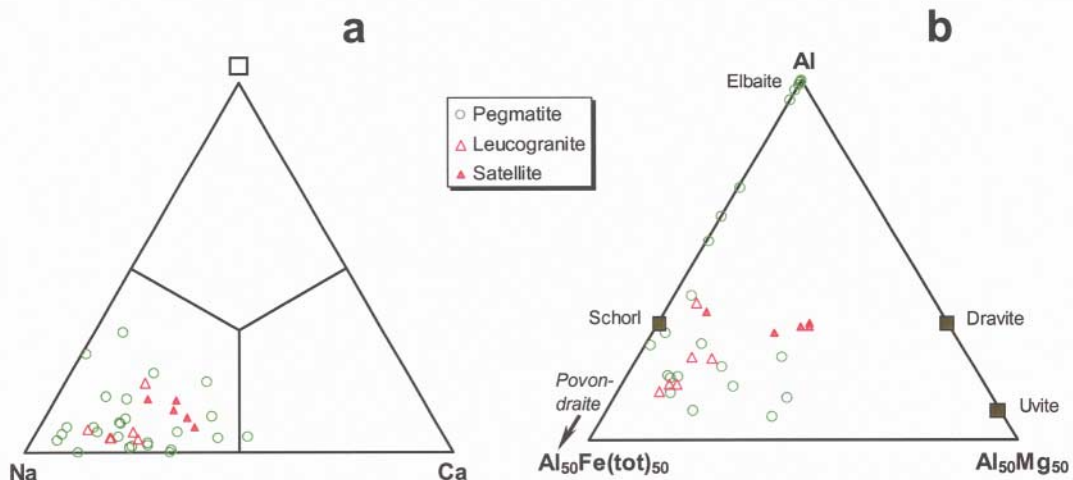


FIG. 9. Plots of tourmaline compositions (after Selway *et al.* 1999). Most points for pegmatite-hosted tourmaline come from pockets. All data points within the formal bounds for schorl and elbaite represent lithium pegmatite.

$$\text{PC1} = -0.04\text{Al} + 0.26\text{Fe}^{3+} + 0.05\text{Ti} + 0.003\text{V} \\ + 0.25\text{Mg} + 0.76\text{Fe}^{2+} - 0.05\text{Mn} - 0.50\text{Li} \\ - 0.005\text{K} - 0.18\text{F} - \alpha_1 \text{ (apfu)}$$

$$\text{PC2} = -0.24\text{Fe}^{3+} - 0.007\text{V} - 0.82\text{Mg} \\ + 0.46\text{Fe}^{2+} + 0.04\text{Mn} + 0.15\text{Li} + 0.11\text{Na} - \\ 0.002\text{K} - 0.12\text{Ca} - \alpha_2 \text{ (apfu)}$$

where α_1 and α_2 are constants, and all eigenvectors of zero value have been removed.

Figure 10 illustrates a plot of the second principal component *versus* the first, and our interpretation of the plot. Tourmaline from leucogranite and satellite dykes varies from dravite–uvite to schorl in composition. Most variation among the samples from satellitic dykes could be due to Mg contamination from metapelitic country-rocks; hence the field for the satellitic dykes is more Mg-enriched than its inferred granitic parent. In its compositional evolution, tourmaline from pegmatite is initially similar to tourmaline from the former grouping; however, in addition to enrichment in (Na, Fe²⁺) at the expense of (Ca, Mg), the tourmaline from pegmatite also becomes enriched in Z-site aluminum and depleted in Fe³⁺. This first leg of the evolutionary history for pegmatite-hosted tourmaline is then followed by considerable enrichment in Li, Al, Mn and F, and elimination of Mg, Ti and V, which takes place only in Li-enriched pockets. In addition, a very late and slight enrichment in Ca takes place in pockets; the local behavior observed for zoned crystals clearly parallels the broader picture. Not only can the principal components analysis be interpreted realistically, it also provides a sense of the rela-

tive timing in enrichment of both major and minor elements.

Recently, Tindle *et al.* (2002) developed methods to assess fractionation *versus* contamination effects (fluid exchange, assimilation) for petalite-subtype pegmatites in northwestern Ontario. Generally, in this region of Ontario, contamination of pegmatite-forming melts by predominantly more mafic host-rocks is expressed by elevated (Mg + Ti + Ca) contents of tourmaline, and the degree of magmatic fractionation is expressed by increased (Li + Mn) contents. Contamination by granitic host-rocks produces very little variation in (Mg + Ti + Ca), whereas contamination by mafic host-rocks produces considerable variation in these elements. Whereas the arguments presented by Tindle *et al.* (2002) seem justified for the petalite-subtype pegmatites in their host terranes in northwestern Ontario, they do not apply well to the pegmatites of the O'Grady batholith. For example, levels of (Mg + Ti + Ca) for "uncontaminated" pegmatite-hosted tourmaline from the O'Grady batholith (Fig. 11) are comparable to, or even exceed, those for samples from northwestern Ontario pegmatites that represent *high degrees* of interaction between pegmatite and host (*e.g.*, exocontact tourmaline and tourmaline directly associated with mafic selvages within pegmatite). This is in spite of the fact that the hosts to the pegmatites of the O'Grady batholith are pegmatitic granite and hornblende granite, *i.e.*, *much less* mafic and reactive than the hosts to the northwestern Ontario pegmatites, and that the tourmaline samples from the O'Grady batholith were not part of assemblages indicative of pegmatite – host-rock interaction. Furthermore, most of the trend

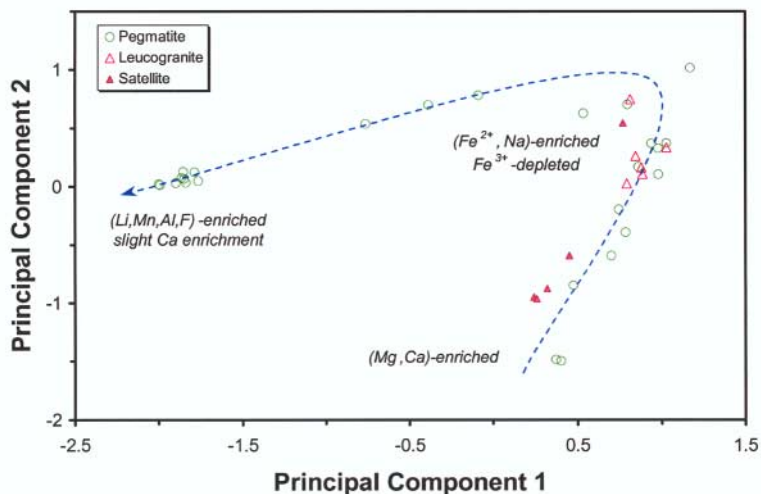


FIG. 10. Principal components analysis chemical variation in tourmaline. The fractionation vector and its interpretation are derived from the component loadings. Note that the vector applies only to granite- and pegmatite-hosted tourmaline. Tourmaline from satellite dykes would seem to be enriched in Mg *via* contamination by host rocks.

indicated by Tindle *et al.* (2002) to account for crystal–melt fractionation is expressed only by pocket tourmaline at the O'Grady batholith (*i.e.*, fractionation involving crystallization from a late hydrous fluid). In conclusion, for the O'Grady batholith, we interpret the more calcic and magnesian composition of tourmaline to have little to do with *in situ* contamination of the melts parental to the pegmatitic granite, and everything to do with the more calcic and magnesian nature of the melts parental to the batholith.

Finally, the strong similarity of Figures 10 and 11 must be pointed out. Rotation of Figure 10 by 180° produces a plot nearly identical to Figure 11. The similarity underscores the usefulness of principal components analysis when working with multidimensional systems, particularly where element covariation and system controls are poorly understood. The ordinate and abscissa variables of Figure 11 were devised by Tindle *et al.* (2002) after 2500 analyses of tourmaline samples were obtained and 32 plots were made and examined. We arrived at Figure 10 completely independently of Tindle *et al.* (2002), after a single, relatively simple set of calculations based on a small sampling.

Micas

Although micas are present in all major lithologies, they are only common in leucogranite and pegmatite. Biotite is the only mica present in the hornblende granite, and is rare in hornblende granite in the vicinity of the lithium-mineralized region. It is a common accessory mineral in the leucogranite, less common in NYF

pegmatite, and absent in lithium-enriched pegmatite. Biotite shows moderate amounts of Mg–Fe zoning; results of an analysis of biotite from pegmatite are given in Table 3.

Muscovite is rare to absent in pegmatite, and lepidolite is uncommon to common, predictably present only in lithium pegmatite. Also present as a pocket phase in lithium pegmatite is an as-of-yet undefined mica with the composition $(\text{Cs,K})_{1-x}(\text{Li,Al})_{3-y}(\text{Si,Al})_4(\text{F,OH})_2$ that can be viewed either as the trioctahedral (Li,F)-analogue of nanpingite or the Cs analogue of lepidolite. The mineral occurs as a late primary pocket phase, associated with colorless elbaite (Fig. 5c), or as a pervasive product of the hydrothermal alteration of pocket K-feldspar (Fig. 5d). It is most commonly found in this latter mode of occurrence; we have yet to encounter a pocket K-feldspar crystal from lithium pegmatite *without* some of this phase. In texture and color (colorless to very pale green), it very much resembles “sericitization”, and without electron imaging or chemical analysis could easily go unnoticed.

Amphibole

Amphibole contents of the hornblende granite are variable, averaging 12 modal %. Samples within a 2-km radius of the lithium-mineralized region show only minor variations in composition, and straddle the boundary between (fluorian ferroan) edenite and magnesio-hornblende. Samples of hornblende granite fulfill criteria for successful use of the Al-in-hornblende barometer (Schmidt 1992, Holland & Blundy 1994,

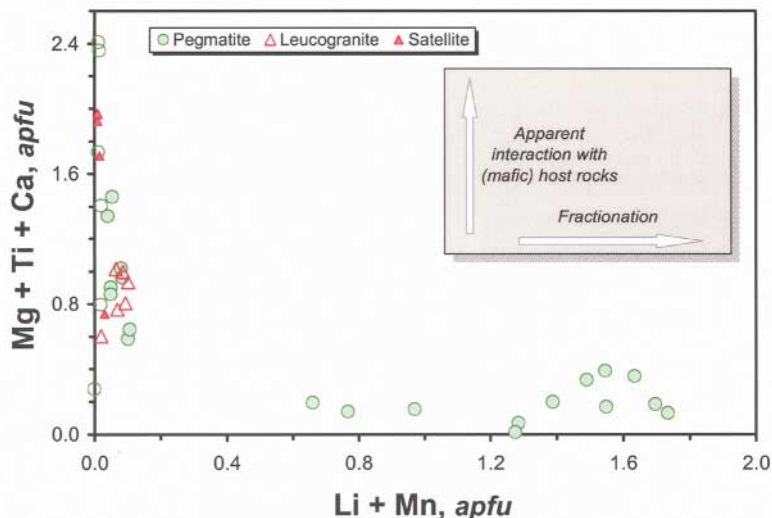


FIG. 11. Plot of Mg + Ti + Ca versus Li + Mn in tourmaline samples, O'Grady batholith. Inset: interpretation of data trends according to Tindle *et al.* (2002). Shaded symbols for pegmatite-hosted tourmaline represent samples from pockets.

Anderson & Smith 1995): (i) the full buffering assemblage of hornblende, biotite, plagioclase, orthoclase, quartz, titanite, ilmenite, (melt and fluid); (ii) a good match to the compositional ranges of the calibration datasets, for example, silica-oversaturated, melt $f(\text{O}_2)$ above the QFM buffer (see Discussion, below), and moderate $\text{Fe}^{3+}/\text{Fe}_{\text{TOT}}$ (all > 0.2) and $\text{Fe}_{\text{TOT}}/(\text{Fe}_{\text{TOT}} + \text{Mg})$ (all between 0.40 and 0.65) in hornblende. For baromet-

TABLE 3. COMPOSITION OF SELECTED ACCESSORY SILICATE MINERALS FROM PEGMATITIC GRANITE AND DERIVATIVES

	‡Zircon	†Titanite	Biotite	Muscovite	Lepidolite	†Pollucite	Ferroaxinite
SiO ₂ wt. %	31.02	30.44	37.36	45.09	60.11	47.11	42.21
TiO ₂	0.00	32.98	3.64	0.00	—	—	0.00
SnO ₂	—	0.08	—	—	—	—	—
ZrO ₂	58.83	—	—	—	—	—	—
HfO ₂	1.78	—	—	—	—	—	—
ThO ₂	1.10	—	—	—	—	—	—
UO ₂	5.96	—	—	—	—	—	—
Nb ₂ O ₅	—	0.98	—	—	—	—	—
Ta ₂ O ₅	—	0.59	—	—	—	—	—
B ₂ O ₃ *	—	—	—	—	—	—	6.11
Al ₂ O ₃	0.16	3.03	13.58	40.47	15.67	15.60	17.62
V ₂ O ₅	—	—	0.27	—	—	—	—
Fe ₂ O ₃	—	2.57	—	—	—	—	—
Y ₂ O ₃	0.68	—	—	—	—	—	—
Yb ₂ O ₃	0.10	—	—	—	—	—	—
MgO	—	0.00	10.23	0.07	0.00	—	1.29
MnO	0.00	0.14	0.27	0.00	0.08	—	1.66
FeO	0.07	—	20.06	0.22	0.08	—	9.30
CaO	0.02	27.78	—	0.00	0.00	0.00	19.50
BaO	—	—	0.03	—	—	—	—
Li ₂ O*	—	—	—	—	6.80	—	—
Na ₂ O	—	—	—	—	—	1.34	—
K ₂ O	0.00	—	9.06	11.82	11.61	0.03	0.00
Rb ₂ O	—	—	0.32	0.11	1.01	0.09	—
Cs ₂ O	—	—	0.03	0.00	0.39	33.79	—
F	—	1.02	1.64	0.00	8.66	—	0.00
Cl	—	—	0.27	—	—	—	—
H ₂ O*	—	0.12	3.04	4.63	0.52	—	1.58
O=F,Cl	—	-0.43	-0.75	—	-3.65	—	—
	99.71	99.30	99.05	102.67	101.28	97.95	99.27
<i>Formula contents</i>							
Si <i>afu</i>	0.997	1.000	2.880	2.921	3.900	2.169	4.004
Ti	0.000	0.815	0.211	0.000	—	—	0.000
Sn	—	0.001	—	—	—	—	—
Zr	0.921	—	—	—	—	—	—
Hf	0.016	—	—	—	—	—	—
Th	0.008	—	—	—	—	—	—
U	0.043	—	—	—	—	—	—
Nb	—	0.015	—	—	—	—	—
Ta	—	0.005	—	—	—	—	—
B	—	—	—	—	—	—	1.000
Al	0.006	0.117	1.234	3.089	1.198	0.847	1.970
V	—	—	0.017	—	—	—	—
Fe ³⁺	—	0.064	—	—	—	—	—
Y	0.012	—	—	—	—	—	—
Yb	0.001	—	—	—	—	—	—
Mg	—	0.000	1.176	0.007	—	—	0.182
Mn	0.000	0.004	0.018	0.000	0.004	—	0.133
Fe ²⁺	0.002	—	1.293	0.012	0.004	—	0.738
Ca	0.001	0.978	—	0.000	0.000	0.000	1.982
Ba	—	—	0.001	—	—	—	—
Li	—	—	—	—	1.774	—	—
Na	—	—	—	—	—	0.119	—
K	0.000	—	0.891	0.977	0.961	0.002	0.000
Rb	—	—	0.016	0.009	0.042	0.003	—
Cs	—	—	0.001	—	0.011	0.663	—
	2.006	2.998	7.737	7.037	7.958	3.802	10.009
F	—	0.106	0.400	0.000	1.777	—	0.000
Cl	—	—	0.035	—	—	—	—
OH	—	0.026	1.565	2.000	0.223	—	1.000
O	4.000	4.868	10.000	10.000	10.000	12.000	15.000
	4.000	5.000	12.000	12.000	12.000	12.000	16.000

‡ average of 4; † average of 2.

ric calculations, the Anderson & Smith (1995) modification of the Schmidt (1992) and Johnson & Rutherford (1989) calibrations was used. As the Anderson & Smith (1995) formulation is partly temperature-dependent, estimates of temperature were derived from the amphibole–plagioclase thermometer of Holland & Blundy (1994), more specifically, the edenite–tremolite calibration for silica-saturated rocks. Furthermore, as the amphibole–plagioclase thermometer is partly pressure-dependent, both sets of calculations were necessarily iterated to mutual consistency. The results shown in Figure 12 represent nine amphibole–plagioclase pairs representing three separate locations. The data points are distributed approximately linearly, with apparent temperatures and pressures ranging from 745°C and 2.9 kbar to 885°C and -0.7 kbar, thus, cursorily, would seem not to have a realistic interpretation. However: (i) in some cases, compositions of *magmatic* plagioclase in direct contact with amphibole could not be determined owing to partial propylitic alteration of plagioclase rims; consequently, plagioclase compositions back of the rims were used in some calculations; (ii) when the data are inspected carefully, amphibole compositions are seen to be relatively constant, whereas the compositions of corresponding plagioclase pairs are apparently variable (Fig. 12); (iii) only samples with relatively highly calcic plagioclase give unrealistic results, with negative pressures; (iv) most data points cluster in a small region with realistic pressures and temperatures and with relatively sodic compositions of plagioclase. We interpret the results as indicating that some of the pairs used in the calculations were not in equilibrium, most likely owing to use of more calcic plagioclase compositions representing areas back of rims abutting hornblende. If

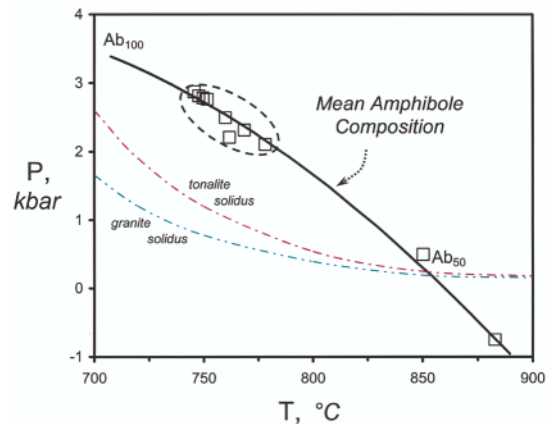


FIG. 12. Results of Al-in-hornblende barometry and hornblende–plagioclase thermometry for samples of hornblende granite. The solid curve is for the mean composition of hornblende coexisting with plagioclase.

these calcic compositions are ignored and only data in the cluster of Figure 12 are used, the mean result for the crystallization of the hornblende granite is $P = 2.5(3)$ kbar, $T = 758(11)^\circ\text{C}$ (note that for the Al-in-hornblende barometer, the standard error of estimation of P is ± 0.6 kbar).

Selected accessory minerals

Zircon is one of the most widely distributed accessory minerals in the O'Grady batholith, and is found in all major units. Samples from granitic pegmatite are richer in U, Th than samples from other units, and are only slightly more Hf-enriched than those from other units (Tables 3, 4), indicating that significant fractionation of Zr versus Hf did not take place at any stage of the crystallization history of the batholith. Core-to-rim variations in zircon composition mimic the general geochemical evolutionary trend: rims are generally more enriched in actinides, lanthanons and Hf than cores; however, some crystals show oscillatory zoning with respect to actinides.

TABLE 4. COMPOSITION OF SELECTED ACCESSORY MINERALS FROM HORNBLENDE GRANITE

	*Zircon	†Thorite	‡Ilmenite	§Scheelite
MoO ₃ wt. %	—	—	—	1.94
WO ₃	—	—	—	77.69
P ₂ O ₅	0.21	3.52	—	—
Nb ₂ O ₅	—	—	0.07	—
SiO ₂	32.26	12.24	—	—
TiO ₂	0.00	0.79	51.91	—
ZrO ₂	64.72	—	—	—
HfO ₂	1.59	—	—	—
ThO ₂	0.20	61.70	—	—
UO ₂	1.18	4.02	—	—
Al ₂ O ₃	—	1.95	—	—
Fe ₂ O ₃	0.18	2.19	0.99	—
Y ₂ O ₃	0.16	0.00	—	—
MnO	—	0.10	1.91	—
FeO	—	—	44.82	—
CaO	0.01	1.31	—	19.60
	100.50	87.82	99.70	99.22
<i>Formula contents</i>				
Mo <i>apfu</i>	—	—	—	0.039
W	—	—	—	0.961
P	0.005	0.169	—	—
Nb	—	—	0.001	—
Si	0.993	0.696	—	—
Ti	0.000	0.034	0.989	—
Zr	0.971	—	—	—
Hf	0.014	—	—	—
Th	0.001	0.798	—	—
U	0.008	0.051	—	—
Al	—	0.131	—	—
Fe ³⁺	0.004	—	0.019	—
Y	0.003	0.000	—	—
Mn	—	0.005	0.041	—
Fe ²⁺	—	—	0.950	—
Ca	0.000	0.080	—	1.002
	2.000	2.056	2.000	2.002
O	4	4	3	4

* average of 7; † average of 3; ‡ average of 2.

Titanite is as widely distributed as zircon, but shows a wider range of compositional variability. Titanite from hornblende granite is significantly more enriched in lanthanons than titanite from either leucogranite or pegmatite, and is more depleted in Mn and Fe. Titanite from hornblende granite and leucogranite shows similar low degrees of enrichment in (Nb + Ta), whereas titanite from pegmatite is significantly more enriched in (Nb + Ta). Titanite from leucogranite and granitic pegmatite achieves only modestly higher degrees of enrichment of Ta relative to Nb than that in the hornblende granite: mean Nb/Ta (hornblende granite) = 4.3, mean Nb/Ta (granite) = 3.2, mean Nb/Ta (pegmatite) = 2.9.

We examined the pattern of intracrystalline zoning in titanite from hornblende granite and leucogranite in some detail. Although the titanite from leucogranite is generally unzoned, titanite from hornblende granite shows compositional zoning. Core-to-rim traverses for titanite from hornblende granite consistently show: (i) an increase in F content and in Mn/(Mn + Fe), and (ii) a decrease in the total lanthanon content, in the ratio of *HREE/REE*, and in total (Nb + Ta). In comparison to the broader geochemical trend displayed among rock types, an important deviation can be detected. Titanite is the main carrier of Ta and Nb in hornblende granite; as such, the consistent trend in zoning toward decreasing (Nb + Ta) with crystallization might indicate that mineral/melt distribution coefficients for (Nb + Ta) of hornblende-granite-hosted titanite are less than 1. If so, the trend later reverses itself, as evidenced by the eventual, local appearance of scarce (Nb, Ta) oxide minerals in pegmatite. This provides a possible explanation for one of the trademark features of the elbaite subtype of rare-element pegmatite: in addition to source characteristics, the typically low contents of Ta and Nb in pegmatites of the subtype might be due to titanite fractionation during the crystallization of melts sequentially parental to the pegmatites.

Scheelite is a rare accessory phase found in hornblende granite, leucogranite and pegmatite. Not previously recognized from the O'Grady batholith, its presence in many rock types accounts for the anomalously high values of tungsten in stream sediment and water samples from the western part of the batholith (Goodfellow 1982). No significant differences seem to exist in the composition of scheelite. Minor intracrystalline zoning exists, with the core more enriched in Mo.

Axinite-group minerals are relatively common accessory phases in the various constituents of the pegmatitic granite. They are contra-indicative of lithium mineralization, as they are found extensively in pegmatite outside of the lithium-mineralized region, and in pegmatite barren of Li minerals inside the region. In all samples analyzed to date, the species present is ferro-axinite. The Mg:Fe ratio varies only slightly, but the Fe:Mn ratio varies from 6 to 2. In general, axinite-group minerals are rarely associated with pegmatites of the elbaite sub-

type. Their presence is most likely due to unusually high activity of Ca in some pegmatite-forming melts, whether for reasons of contamination (*e.g.*, skarns and marbles in the case of pegmatites of the Moldanubicum, M. Novák, pers. commun.), or for reasons simply involving the presence of more calcic melts, such as those parental to the O'Grady batholith.

Y, REE minerals. Lanthanons are dispersed among a diverse assemblage of silicate, phosphate and oxide minerals: zircon, titanite, epidote-group minerals, pyrochlore-group minerals, fergusonite-(Y), xenotime-(Y) and monazite-(Ce). Of the major carriers of lanthanon elements (Table 5), epidote-group minerals are the most common (allanite subgroup); all other species are extremely rare. Allanite-subgroup minerals are present in all major lithologies, but are most obvious in pegmatite, occurring only in bodies of NYF affinity, as euhedral crystals to 4 cm in length. Two species were encountered in samples from the batholith: allanite-(Ce) and rare allanite-(La). The samples show extreme degrees of *LREE* enrichment, second only to monazite samples (Fig. 13). Pyrochlore-group minerals show approximately flat chondrite-normalized *REE* patterns, whereas xenotime-(Y) and fergusonite-(Y) show strongly *HREE*-enriched patterns. All display some degree of kinking in their patterns, particularly in the vicinity of Sm, where the *REE* in allanite first become undetectable with an electron microprobe. Given the relative abundance of allanite-subgroup minerals and their presence in all major rock-types, it is tempting to

suggest that kinking in the chondrite-normalized patterns for the other major carriers of the *REE* is due to the earlier fractionation of allanite-subgroup phases.

Nb-Ta oxide minerals. Although some oxide minerals are carriers of Nb and Ta, *e.g.*, rutile and ilmenite (and its alteration product pseudotitane: Table 6), few true occurrences of (Nb,Ta)-oxide minerals exist at O'Grady. Despite their extremely low absolute abundance, niobium and tantalum are carried by an impressively diverse number of species at O'Grady, including stibicolumbite, four species of the pyrochlore group and fergusonite-(Y). Pyrochlore-group species encountered to date are: pyrochlore, ytropyrochlore-(Y), plumbopyrochlore and the extremely rare species bismutopyrochlore (Tables 5, 6). The most common occurrence of pyrochlore-group minerals is in pegmatite, typically as octahedral crystals of pyrochlore (*sensu stricto*) in pockets. These pyrochlore crystals show evidence of late-stage (hydrothermal) replacement by hydrous bismuthian plumbopyrochlore (Fig. 5b). Bismutopyrochlore has been found in only one sample from the satellitic dykes. Mildly uranoan ytropyrochlore-(Y) has been found as only one crystal in one sample of leucogranite. Stibicolumbite occurs as extremely rare, euhedral opaque black crystals to 0.5 mm.

TABLE 5. COMPOSITION OF SELECTED PYROCHLORE-GROUP PHASES AND *REE* MINERALS FROM PEGMATITIC GRANITE AND DERIVATIVES

	Fergusonite (-Y)	Ytropyrochlore-(Y)	Bismuto- pyrochlore	Allanite (-Ce)	Monazite (-Ce)	Xeno- time-(Y)
P ₂ O ₅ , wt.%	—	—	—	—	28.25	32.79
Nb ₂ O ₅	37.08	31.90	13.70	—	—	—
Ta ₂ O ₅	1.50	18.76	10.47	—	—	—
SiO ₂	—	4.53	10.54	30.11	1.38	1.92
TiO ₂	3.12	1.06	1.88	1.59	0.00	0.00
ZrO ₂	—	—	0.41	—	—	—
ThO ₂	3.06	1.29	8.24	1.39	5.65	0.65
UO ₂	8.76	5.96	3.54	0.00	0.44	1.14
Al ₂ O ₃	0.07	0.50	2.17	12.57	0.17	0.06
Fe ₂ O ₃	0.89	0.97	0.24	4.25	—	—
Y ₂ O ₃	21.18	6.67	0.52	0.00	1.89	43.57
La ₂ O ₃	0.13	0.30	0.48	9.84	13.55	—
Ce ₂ O ₃	0.73	0.78	1.74	11.04	29.17	0.08
Pr ₂ O ₃	0.18	0.11	0.26	0.70	3.36	0.18
Nd ₂ O ₃	1.68	0.57	0.81	1.41	12.52	0.35
Sm ₂ O ₃	1.47	0.47	0.35	—	2.50	1.12
Gd ₂ O ₃	2.64	0.67	0.29	—	1.43	2.82
Tb ₂ O ₃	0.53	—	0.08	—	0.16	0.65
Dy ₂ O ₃	4.05	—	0.61	—	0.59	5.32
Ho ₂ O ₃	0.83	—	0.09	—	0.07	1.22
Er ₂ O ₃	2.40	—	0.17	—	0.10	3.95
Tm ₂ O ₃	0.33	—	0.03	—	—	0.53
Yb ₂ O ₃	2.21	—	0.24	—	—	4.74
Lu ₂ O ₃	0.30	—	0.04	—	—	0.52
Bi ₂ O ₃	—	—	25.60	—	—	—
MnO	0.00	0.00	—	0.50	0.00	0.00
FeO	—	—	—	11.73	0.32	0.00
CaO	0.86	5.65	1.63	10.66	0.25	0.15
SnO	—	0.00	—	—	—	—
PbO	0.00	4.40	3.16	—	0.00	0.00
Na ₂ O	0.05	—	0.00	—	0.00	0.00
H ₂ O*	—	—	—	1.48	—	—
	94.05	84.59	87.29	97.27	101.80	101.76

* calculated for stoichiometry; odd numbered REE in italics by interpolation; † average of 6. In the case of allanite, Fe²⁺:Fe³⁺ calculated according to stoichiometry.

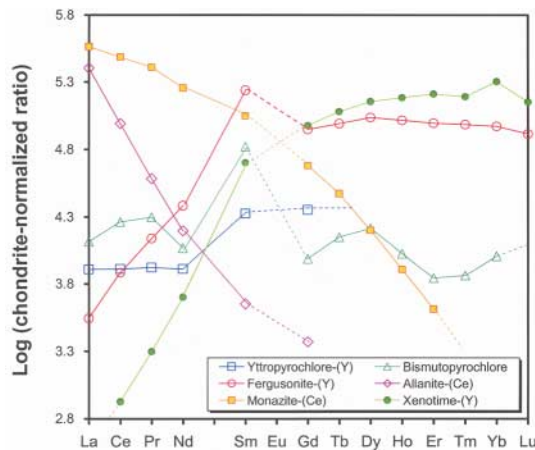


FIG. 13. Chondrite-normalized *REE* plots for accessory minerals of the pegmatitic granite and its pegmatites. Odd-numbered *REE* are interpolated, except for xenotime-(Y). Only pyrochlore-group minerals show significant kinking, presumably owing to earlier fractionation of an allanite-subgroup phase. The dashed line in the vicinity of Eu indicates that Eu was undetected, not that it is absent.

It is unusual in that it seems to be the example richest in Nb, W and Pb²⁺ of the species to date (Table 6). Fergusonite-(Y) occurs only as a single grain in one sample of leucogranite. As is typical for the species, it shows a strong structural preference for Nb over Ta. The suite of (Nb,Ta)-oxide minerals shows consistently very low levels of Ta enrichment, the *apparent* exception being pyrochlore-group minerals that, in granitic melts, accommodate Ta in preference to Nb (Ericit 1998).

DISCUSSION

That the lithium pegmatites of the O'Grady batholith represent the elbaite subtype is unambiguous. Elbaite is the dominant carrier of lithium; lepidolite is a distant second, and has a composition close to polyolithionite. Typomorphic accessory minerals follow the proscribed behavior: danburite (common) and hambergite (uncommon) are present; topaz, amblygonite–montebrasite and petalite are absent (Table 1). Tourmaline is enriched in Mn and F, and has relatively high X-site Ca and a low proportion of X-site vacancies. Quantities of accessory minerals of P, Ta and Nb are minor (scarce at O'Grady). All of the above are key features of the elbaite subtype (Novák & Povondra 1995).

In their defining paper on the elbaite subtype, Novák & Povondra (1995) stated that the relationship between most examples of the elbaite subtype and their granitic "parents" is not clear. The O'Grady batholith potentially offers a rare glimpse of much of the fractionation history preceding the formation of pegmatites of the elbaite subtype. That the hornblende granite and leucogranite sequentially represent previous products of crystallization *en route* to the lithium pegmatites is unambiguous:

(i) Field relations and geochronological data indicate that the hornblende granite and pegmatitic granite are contemporaneous.

(ii) The hornblende granite is anomalously rubidium-enriched, and shows elevated and highly variable levels of boron, making it a suitable precursor to the pegmatitic granite. Values of K/Rb for the only volumetrically significant carrier of Rb (K-feldspar) vary continuously from hornblende granite to leucogranite to pegmatite.

(iii) Plagioclase compositions for leucogranite and pegmatite are, on the whole, more calcic than is typical for LCT-type pegmatite and its granite precursors, but one would expect this if hornblende granite were the product of fractionation to directly precede the leucogranite. In addition, compositional gaps shown by plagioclase in the hornblende granite are also expressed by plagioclase in the pegmatitic granite (both leucogranite and pegmatite). The anomalously calcic nature of plagioclase is a typical feature of Selwyn-suite plutons (two-mica plutons: An₂₂ to An₅₆; hornblende-bearing plutons: An₂₈ to An₅₇; transitional plutons: An₂₅ to An₆₄; Gordey & Anderson 1993). The core zone of plagioclase crystals from Selwyn-suite plutons is locally

highly calcic, skeletal and altered, suggestive of magma mixing; however, resolution of these and related issues requires further and broader study of the O'Grady batholith and other Selwyn suite plutons.

(iv) The accessory mineralogy of the hornblende granite is remarkably comparable to that of leucogranite and pegmatite. Furthermore, the chemical composition, occurrence and abundance of hornblende, zircon, titanite, scheelite and lanthanon minerals are consistent with the inferred sequence of fractionation.

The inferred evolution of the batholith reinforces the proposal by Novák & Povondra (1995) that the elbaite subtype has its origins with a much more alkaline par-

TABLE 6. COMPOSITION OF SELECTED NONSILICATE MINERALS FROM PEGMATITIC GRANITE AND DERIVATIVES

	*Ilmenite	Pseudo-rutile	Rutile	†Mag-netite	‡Stibio-columbite	§Pyro-chlore	Scheelite
MoO ₃ wt. %	—	—	—	—	—	—	2.35
WO ₃	—	—	0.29	—	9.67	2.78	77.48
Nb ₂ O ₅	0.27	0.93	11.22	0.00	38.58	58.61	—
Ta ₂ O ₅	0.00	0.00	0.08	0.00	1.13	8.09	—
SiO ₂	—	1.42	—	—	—	—	—
TiO ₂	48.34	66.21	82.81	0.08	—	0.36	—
SnO ₂	—	—	0.17	—	—	—	—
UO ₂	—	—	—	—	—	2.93	—
Al ₂ O ₃	—	0.58	—	—	—	—	—
Fe ₂ O ₃	7.71	25.27	4.02	69.03	0.00	0.00	—
Sb ₂ O ₃	—	—	—	—	42.40	0.00	—
Bi ₂ O ₃	—	—	—	—	1.13	0.00	—
MgO	0.03	0.04	—	0.00	—	—	—
MnO	5.54	0.60	0.17	0.00	0.00	—	—
FeO	38.09	—	4.77	31.20	—	—	—
CaO	0.00	0.26	—	0.00	—	12.50	19.98
SnO	—	—	—	—	0.29	1.23	—
PbO	—	—	—	—	7.04	0.00	—
Na ₂ O	—	—	—	—	—	7.50	—
H ₂ O	—	4.46	—	—	—	0.15	—
F	—	—	—	—	—	4.38	—
O=F	—	—	—	—	—	-1.84	—
	99.98	99.76	99.92	100.31	100.24	96.68	99.81
	<i>Formula contents</i>						
Mo <i>apfu</i>	—	—	—	—	—	—	0.047
W	—	—	0.002	—	0.125	0.049	0.950
Nb	0.003	0.029	0.142	0.000	0.866	1.785	—
Ta	0.000	0.000	0.001	0.000	0.015	0.148	—
Si	—	0.096	—	—	—	—	—
Ti	0.922	3.348	1.738	0.002	0.000	0.018	—
Sn ⁴⁺	—	—	0.002	—	—	—	—
U	—	—	—	—	—	0.044	—
Al	—	0.046	—	—	—	—	—
Fe ²⁺	0.147	1.279	0.084	1.995	0.000	0.000	—
Sb ³⁺	—	—	—	—	0.868	0.000	—
Bi ³⁺	—	—	—	—	0.015	0.000	—
Mg	0.001	0.004	—	0.000	—	—	—
Mn	0.119	0.034	0.004	0.000	0.000	—	—
Fe ²⁺	0.808	—	0.027	1.003	—	—	—
Ca	0.000	0.019	—	0.000	—	0.902	1.012
Sn ²⁺	—	—	—	—	0.007	0.037	—
Pb	—	—	—	—	0.094	—	—
Na	—	—	—	—	—	0.980	—
	2.000	4.852	2.000	3.000	1.989	3.963	2.008
OH	—	2	—	—	—	0.067	—
F	—	—	—	—	—	0.933	—
O	3	8	4	4	4	6	4

* average of 3; † average of 2; ‡ average of 6; H₂O and Fe²⁺:Fe³⁺ calculated on the basis of stoichiometry.

ent medium than other subtypes of rare-element pegmatites of LCT lineage.

Barometric analysis of the hornblende granite indicates that the main mass of the O'Grady batholith crystallized at depths corresponding to $P = 2.5$ kbar. These results agree qualitatively with other observations for the O'Grady batholith and its Selwyn suite neighbors: (i) many of the plutons are associated with tungsten skarns, which are typically indicative of intermediate depths in the crust (Einaudi *et al.* 1981), (ii) members of the Selwyn suite in the Nahanni and Nidderly Lake map areas (NTS 105 I, O) typically have a relatively wide contact-aureole and show no chilled marginal facies at their contacts (Anderson 1982, Duncan 1999). As the data points of Figure 12 lie above the solidi for H_2O -saturated granite and tonalite, we infer that at the melts parental to the hornblende granite were not H_2O -saturated at the time of hornblende crystallization (*cf.* Anderson & Smith 1995). Along this line, it is interesting that the inferred depth of crystallization is in the vicinity of the critical depth for separation of a magmatic volatile phase (pressures of 2.5 kbar: Candela & Blevin 1995). The absence of miarolitic textures in the hornblende granite indicates either that initial H_2O contents of its parental magma were too low for the establishment of connected volumes of a volatile phase (prerequisite for efficacious transport of the volatile phase, and subsequent formation of hydrothermal mineral deposits), or that the crystallization pressure was too high, resulting in dispersal of the volatile phase among existing products of crystallization (resulting in partial propylitization of feldspars and amphiboles). However, a more hydrous melt, represented by the pegmatitic granite, did eventually separate and crystallize in the upper portions of the hornblende granite. On the basis of the boron- and volatile-rich leucocratic composition of the pegmatitic granite, we infer that its crystallization took place at much lower temperatures than the hornblende granite, but not necessarily at much lower pressures (*cf.* Candela & Blevin 1995, Černý 1991).

On the basis of the mineralogical and geochemical criteria, it is also evident that the dykes satellitic to the O'Grady batholith are merely finer-grained equivalents of the pegmatitic granite, differing only in ways that are a function of the lower ambient temperatures outside of the batholith at the time of crystallization, and by minor assimilation of country rocks. Unfortunately, accounts of the nature of the external dykes are not consistent; Anderson (1983) described both felsitic and pegmatitic dykes, Gordey and Anderson (1993) described only felsitic dykes, and we have encountered only felsitic dykes. Whether external dykes of pegmatite are actually present is a question that we found financially too prohibitive to answer in this remote and rough terrain.

A feature not recognized before for the elbaite subtype and its magmatic parents is crystallization at elevated $f(O_2)$. That the O'Grady melts crystallized mostly under $f(O_2)$ conditions in excess of the QFM buffer is

underscored by the accessory phase assemblage magnetite – titanite – allanite – apatite – zircon (Wones 1989, Robinson & Miller 1999) in hornblende granite, leucogranite and NYF pegmatite, and by the anomalously Fe^{3+} -rich and subaluminous composition of tourmaline. That elevated $f(O_2)$ is not due to country-rock "contamination" (*cf.* Novák & Povondra 1995) is shown by the satellitic dykes, which are devoid of magnetite and host tourmaline with significantly lower $Fe^{3+}:Fe^{2+}$ ratios than tourmaline from granite (Fig. 9b). It is unlikely that elevated $f(O_2)$ during most of the crystallization history of the O'Grady batholith is attributable to degassing of magma emplaced at shallow levels in the crust: (i) geobarometry indicates that the main mass of the batholith crystallized at moderate depths; (ii) stable isotope analysis, compositional data for hydrous phases and thermal evolutionary models for the nearby Emerald Lake pluton, a geochemically similar, Tombstone-suite sister of the O'Grady batholith in a similar emplacement setting (Coulson *et al.* 2002), indicate that low amounts of magma degassing took place during its crystallization history. Thus, by analogy, low levels of magma degassing might be expected for the melts parental to the O'Grady batholith. In conclusion, the elevated $f(O_2)$ of melts parental to the O'Grady batholith would most likely seem to be attributable to pre-emplacment conditions and events surrounding the generation of the parental melt.

The mixed geochemical characteristics of the broader Selwyn plutonic suite have led to a variety of models to explain their genesis: subduction-related melting (Gabrielse & Yorath 1992), crustal thickening and melting associated with convergent tectonics (Woods-worth *et al.* 1992, Gordey & Anderson 1993), and contamination of mantle-derived melts with old, radiogenically undepleted crust (Coulson *et al.* 2000). That these mixed characteristics carry through to the pegmatite-forming stage at the O'Grady batholith is unequivocal: over most of the 10-km belt of pegmatitic granite, pegmatites show a mild NYF signature (they are allanite-, biotite- and magnetite-bearing), yet locally achieve a level of fractionation that is distinctly LCT-like in composition (elbaite, lepidolite, pollucite, elevated Rb and Cs levels of K-feldspar), a rare combination for pegmatite fields. Although it is clearly beyond the scope of the present study to establish, much less speculate, on the petrogenesis of the Selwyn plutonic suite, the study certainly illustrates some of the challenges associated with the derivation of petrogenetic models for the suite.

CONCLUSIONS

1) The lithium pegmatites of the O'Grady batholith are the first reported Canadian occurrence of the elbaite subtype of rare-element pegmatite. The composition of the main and accessory minerals consistently indicates that the hornblende granite is the direct precursor to

pegmatitic granite and pegmatite. Felsitic dykes satellitic to the batholith are external equivalents to the leucogranitic portions of the system.

2) The melts parental to the pegmatites were more voluminous and alkaline, and less aluminous and reduced, than is usual for melts parental to LCT-type rare-element pegmatites. These characteristics would seem to have an expression that carries through to the pegmatite stage. The vast majority of pegmatites have a mild NYF signature, and only locally attain a level of fractionation showing an LCT signature.

3) We found field indicators of lithium mineralization and pockets not previously recognized for pocket pegmatite occurrences, nor for the elbaite subtype. The presence of axinite-group minerals is contra-indicative of Li-mineralized pockets in the O'Grady batholith. Otherwise pink or white K-feldspar is occasionally bluish green (amazonitic) in the immediate vicinity of Li-mineralized pockets.

4) Because of the relatively young mid-Cretaceous age of the batholith, its evolution can be monitored *via* Rb–Sr fractionation, which is generally not possible with older pegmatite–granite systems.

5) The main phases of the O'Grady batholith and their later differentiates are relatively Ca-rich. This enrichment is recorded in abundant calcic amphibole (hornblende granite), in plagioclase and tourmaline compositions, and in the relative abundance of calcic pocket phases (*e.g.*, danburite). Anomalously calcic compositions of the melt are characteristic of members of the Selwyn plutonic suite, and would seem to have more to do with melt generation than with *in situ* contamination during crystallization (*e.g.*, *via* assimilation of calcic country-rocks).

6) In addition to source characteristics, the role of apatite and titanite fractionation should be considered when assessing the typically low P, Nb and Ta contents of pegmatites of the elbaite subtype.

7) Plots used by Tindle *et al.* (2002) to assess the effects of contamination *versus* fractionation *via* tourmaline chemistry for pegmatites of the petalite subtype of rare-element granitic pegmatite do not seem to be readily applicable to the elbaite subtype.

8) Principal components analysis is a useful way to examine and model the petrochemical evolution of compositionally complex mineral species. Principal components analysis of tourmaline from the O'Grady batholith shows two trends that can be interpreted as: (i) magmatic crystallization producing enrichment in Na, Fe²⁺ and Z-site Al at the expense of Ca, Mg and Fe³⁺, and (ii) crystallization from pocket fluids marked by enrichment in Li, Al, Mn and F, and elimination of Mg, Ti and V. The generally less aluminous nature and higher *f*(O₂) of the melts parental to the O'Grady batholith are expressed in the composition of the tourmaline and other minerals, and by the assemblage of accessory minerals magnetite – titanite – allanite – apatite – zircon in hornblende granite, leucogranite and NYF pegmatite.

9) Thermobarometric analysis implies that the main mass of the O'Grady batholith crystallized mesozonally at less than H₂O-saturated conditions. However, H₂O saturation did occur by the time of crystallization of the pegmatitic granite, as evidenced by the abundance of pegmatite-hosted miarolitic cavities.

ACKNOWLEDGEMENTS

We thank assistants Mark H.F. Mauthner, Sylvie Marcil and Anita Lam for their considerable help in the field, and for some of the photography (MHFM). We also thank Brad Wilson of Alpine Gems for many of the samples used in this study, Petr Černý and Mike Wise for helpful discussions, and Milan Novák and editor Robert F. Martin for thoughtful reviews of the manuscript. Financial support for the project was provided by the Department of Indian Affairs and Northern Development (Yellowknife, N.W.T.), the Canada–Yukon Mineral Development Agreement (Whitehorse, Yukon), by Canadian Museum of Nature RAC grants to TSE, and by NSERC research grants to LAG.

REFERENCES

- ANDERSON, J.L. & SMITH, D.R. (1995): The effects of temperature and *f*O₂ on the Al-in-hornblende barometer. *Am. Mineral.* **80**, 549-559.
- ANDERSON, R.G. (1982): Geology of the Mactung Pluton in Niddery Lake map area and some of the plutons in Nahanni map area, Yukon Territory and District of Mackenzie. *In* Current Research, Part A. *Geol. Surv. Can., Pap.* **82-1A**, 299-304.
- _____ (1983): Selwyn plutonic suite and its relationship to tungsten skarn mineralization, southeastern Yukon and District of Mackenzie. *In* Current Research, Part B. *Geol. Surv. Can., Pap.* **83-1B**, 151-163.
- BURNS, P.C., MACDONALD, D.J. & HAWTHORNE, F.C. (1994): The crystal chemistry of manganese-bearing elbaite. *Can. Mineral.* **32**, 31-41.
- CANDELA, P.A. & BLEVIN, P.L. (1995): Do some miarolitic granites preserve evidence of magmatic volatile phase permeability? *Econ. Geol.* **90**, 2310-2316.
- CECILE, M.P. (1984): Geology of southwest and central Niddery Lake area, Yukon Territory. *Geol. Surv. Can., Open File* **1118**.
- ČERNÝ, P. (1991): Rare-element granitic pegmatites. I. Anatomy and internal evolution of pegmatite deposits. *Geosci. Canada* **18**(2), 49-67.
- CLARK, G.S. & ČERNÝ, P. (1987): Radiogenic ⁸⁷Sr, its mobility, and the interpretation of Rb–Sr fractionation trends in rare-element granitic pegmatites. *Geochem. Cosmochim. Acta* **51**, 1011-1018.

- COULSON, I.M., DIPPLE, G.M., VILLENEUVE, M.E., RUSSELL, J.K. & MORTENSEN, J.K. (2000): Thermal history and timescales of assembly of high-level composite plutons: implications for the origin of the Tombstone Plutonic Suite, Yukon Territory, Canada. *Can. Soc. Expl. Geophys., CSEG Conf. Abstr.* – 2000, 907.
- _____, VILLENEUVE, M.E., DIPPLE, G.M., DUNCAN, R.A., RUSSELL, J.K. & MORTENSEN, J.K. (2002): Time-scales of assembly and thermal history of a composite felsic pluton: constraints from the Emerald Lake area, northern Canadian Cordillera, Yukon. *J. Volcanol. Geotherm. Res.* **114**, 331-356.
- DUNCAN, R.A. (1999): *Physical and Chemical Zonation In The Emerald Lake Pluton, Yukon Territory*. M.Sc. thesis, Univ. British Columbia, Vancouver, British Columbia.
- EINAUDI, M.T., MEINERT, L.D. & NEWBERRY, R.J. (1981): Skarn deposits. *Econ. Geol., 75th Anniv. Vol.*, 317-391.
- ERCIT, T.S. (1998): Tantalum–niobium oxide minerals and pegmatite genesis. *Int. Mineral. Assoc., 17th Gen. Meet. (Toronto)*, A146 (abstr.).
- _____, GROAT, L.A. & GAULT, R.A. (1998): A gem-tourmaline-bearing aplite–pegmatite complex, O'Grady batholith, western N.W.T. *Indian & Northern Affairs Can., N.W.T. Geol. Mapping Div., Open File EGS 1998-09*.
- GABRIELSE, H. & YORATH, C.J. (1992): Tectonic synthesis. In *Geology of the Cordilleran Orogen in Canada* (H. Gabrielse & C.J. Yorath, eds.). *Geol. Surv. Can., Geology of Canada* **4**, 677-705.
- GOODFELLOW, W.D. (1982): Regional stream sediment and water geochemistry of the Nahanni map area (NTS 1051), Yukon and Northwest Territories. *Geol. Surv. Can., Open File* **868**.
- GORDEY, S.P. & ANDERSON, R.G. (1993): Evolution of the northern Cordilleran miogeocline, Nahanni map area (1051), Yukon and Northwest Territories. *Geol. Surv. Can., Mem.* **428**.
- GRICE, J.D. & ERCIT, T.S. (1993): Ordering of Fe and Mg in tourmaline: the correct formula. *Neues Jahrb. Mineral., Abh.* **165**, 245-266.
- GROAT, L.A., ERCIT, T.S., MORTENSEN, J.K. & MAUTHNER, M.H.F. (1995): Granitic pegmatites in the western Northwest Territories. *Indian & Northern Affairs Can., N.W.T. Geol. Mapping Div., Open File EGS 1995-10*.
- HAWTHORNE, F.C. & HENRY, D.J. (1999): Classification of the minerals of the tourmaline group. *Eur. J. Mineral.* **11**, 201-215.
- _____, MACDONALD, D.J. & BURNS, P.C. (1993): Reassignment of cation site occupancies in tourmaline: Al/Mg disorder in the crystal structure of dravite. *Am. Mineral.* **78**, 265-270.
- HEFFERNAN, S. & MORTENSEN, J.K. (2000): Age, geochemical and metallogenic investigations of Cretaceous intrusions in southeastern Yukon and southwestern NWT: a preliminary report. *Yukon Expl. Geol.* 1999, 145-149.
- HOLLAND, T. & BLUNDY, J. (1994): Non-ideal interactions in calcic amphiboles and their bearing on amphibole–plagioclase thermometry. *Contrib. Mineral. Petrol.* **116**, 433-447.
- HUNT, P.A. & RODDICK, J.C. (1987): A compilation of K–Ar ages, Report 17. In *Radiogenic Age and Isotopic Studies, Report 1*. *Geol. Surv. Can., Pap.* **87-2**, 143-210.
- JOHNSON, M.C. & RUTHERFORD, M.J. (1989): Experimental calibration of the aluminum-in-hornblende geobarometer with application to Long Valley caldera (California). *Geology* **17**, 837-841.
- LONDON, D., ČERNÝ, P., LOOMIS, J.L. & PAN, J.J. (1990): Phosphorus in alkali feldspars of rare-element granitic pegmatites. *Can. Mineral.* **28**, 771-786.
- MORTENSEN, J.K., LANG, J.R. & BAKER, T. (1997): Age and gold potential of the Tungsten plutonic suite in the Macmillan Pass area, western N.W.T. *N.W.T. Geosci. Forum, 25th Anniv., Program Abstr., Talks Posters (Yellowknife)*, 79-80.
- NOVÁK, M. & POVONDRA, P. (1995): Elbaite pegmatites in the Moldanubicum: a new subtype of the rare-element class. *Mineral. Petrol.* **55**, 159-176.
- _____, SELWAY, J.B., ČERNÝ, P., HAWTHORNE, F.C. & OTTOLINI, L. (1999): Tourmaline of the elbaite–dravite series from an elbaite-subtype pegmatite at Blizná, southern Bohemia, Czech Republic. *Eur. J. Mineral.* **11**, 557-568.
- PEARCE, J.A. (1996): Sources and settings of granitic rocks. *Episodes* **19**, 120-125.
- _____, HARRIS, N.B.W. & TINDLE, A.G. (1984): Trace element discrimination diagrams for the tectonic interpretation of granitic rocks. *J. Petrol.* **25**, 956-983.
- ROBINSON, D.M. & MILLER, C.F. (1999): Record of magma chamber processes preserved in accessory mineral assemblages, Aztec Wash pluton, Nevada. *Am. Mineral.* **84**, 1346-1353.
- SCHMIDT, M.W. (1992): Amphibole composition in tonalite as a function of pressure: an experimental calibration of the Al-in-hornblende barometer. *Contrib. Mineral. Petrol.* **110**, 304-310.
- SELWAY, J.B., ČERNÝ, P., HAWTHORNE, F.C. & BREAKS, F.W. (1998): Compositional evolution of tourmaline in petalite-subtype pegmatites. *Int. Mineral. Assoc., 17th Gen. Meet. (Toronto)*, *Abstr. Programme*, A148.
- _____, NOVÁK, M., ČERNÝ, P. & HAWTHORNE, F.C. (1999): Compositional evolution of tourmaline in lepidolite-subtype pegmatites. *Eur. J. Mineral.* **11**, 569-584.
- TINDLE, A.G., BREAKS, F.W. & SELWAY, J.B. (2002): Tourmaline in petalite-subtype granitic pegmatites: evidence of

fractionation and contamination from the Pakeagama Lake and Separation Lakes areas of northwestern Ontario, Canada. *Can. Mineral.* **40**, 753-788.

WEIDNER, J.R. & MARTIN, R.F. (1987): Phase equilibria of a fluorine-rich leucogranite from the St. Austell pluton, Cornwall. *Geochim. Cosmochim. Acta* **51**, 1591-1597.

WONES, D.R. (1989): Significance of the assemblage titanite + magnetite + quartz in granitic rocks. *Am. Mineral.* **74**, 744-749.

WOODSWORTH, G.J., ANDERSON, R.G., ARMSTRONG, R.L., STRUIK, L.C. & VAN DER HEYDEN, P. (1992): Plutonic Regimes. In *Geology of the Cordilleran Orogen in Canada* (H. Gabrielse & C.J. Yorath, eds.). *Geol. Surv. Can., Geology of Canada* **4**, 491-531.

Received December 6, 2001, revised manuscript accepted December 13, 2002.

APPENDIX 1



BSE photo-mosaic of leucogranite sample RG319. The textures and mineralogy displayed by this sample are typical of leucogranite in the vicinity of the lithium-mineralized region. Q: quartz, K: K-feldspar, P: plagioclase, S: schorl.